Analysis, Design and Optimization of Navier-Stokes Flows around Interacting Sails

Vincent G. Chapin[1]

Romaric Neyhousser[2], **Guillaume Dulliand**[3], **Patrick Chassaing**[4]

INTRODUCTION

Computational Fluid Dynamics (CFD) which consists to numerically resolve governing equations of fluid motion around any body have been used for sailing yacht design for more than thirty years [8,13]. At the beginning inviscid equations were used with well-known panel codes and singularity methods because computing power was not sufficient to use more realistic viscous model. Drawbacks of these inviscid methods are well known to predict real flows with separated regions and unsteady phenomena [4,5,10,11]. From the beginning of this pioneering period, computing power of personal computers has increased by more than a forty thousand factor following famous Moore's law! On a single processor personal computer, one year of CPU time in 1971 represents twelve minutes today and twenty seconds in ten years.

In aeronautic, viscous CFD are absolutely indispensable to plane designers from wing to engine design. Recently, they have been massively introduced in IACC design for America's Cup with an apparent great success for Alinghi in 2003 [2,3,10].

In the following years, viscous CFD based on Reynolds Averaged Navier-Stokes (RANS) equations, if encapsulated in a friendly environment, should rapidly become an indispensable decision-making tool in competitive sailing yacht analysis, design and optimization [4,5,11]. This is mainly related to three factors. First, as said before, computer power of personal computers always increased along a straight line with an order of magnitude increase each six years. Secondly, progress in design, increase the need for high level tools to understand and enhance aero-hydrodynamic of sailing yachts. From high speed sailing yacht in 1905 with Charlie Barr to high speed sailing yacht in 2001 with Steve Fossett, and a transatlantic record from 12 days to 4 days, progress are considerable. Design methods have evolved a lot. The third factor and perhaps the more important one, from the sail designer point of view, is the better integration of CAD design, mesh generation, flow solver, post-processing and optimization algorithms which is now possible and relatively new. This gives access to these tools to a larger community of designers and sailors without high-level fluid mechanics and numerical methods background. As we will show in the paper, it becomes possible to pose new design questions by using these tools in a more integrated and automated manner. It is not just flow analysis but it becomes rig design or optimization.

This work has been initiated through a partnership between Y. PARLIER design team, their innovative sailing yacht concept: the Hydraplaneur "Médiatis Région Aquitaine" and the Fluid Mechanics Department of ENSICA (Ecole Nationale Supérieure des Ingénieurs de Construction Aéronautique). It has begun by wind-tunnel tests of the aerodynamic performances of the new double rig concept and its comparison with classical rig to help designers to make a choice for Hydraplaneur [6]. Next, we have developed an integrated approach with wind-tunnel tests and RANS-based simulations to investigate in more details the double rig concept and help the validation of the developed viscous CFD technology able to take into account separated and unsteady flows [4,5].

In this paper, we are focusing on the interaction between multiple sails and what can be done to optimize their design, in a constrained environment (deck plan, structural limits, etc…), by using a newly developed integrated and automated computational environment based on RANS simulations and named *ADONF* (Analysis, Design and Optimization of Navier-Stokes Flows).

1 Associate Professor, Fluid Mechanics Department, ENSICA,Toulouse, France
vincent.chapin@ensica.fr, http://high-speed-sailing.site.voila.fr/
2 Naval Architect, Aquitaine Design Team, OCEA, Y. PARLIER
3 Mesh specialist, Fluid Mechanics Department, ENSICA
4 Professor INPT and Fluid Mechanics Department, ENSICA

COMPUTATIONAL MODEL

In this section, main elements of the computational model are described. First the fluid dynamics equations used to simulate the flow around interacting sails are presented then the solver and physical models and limitations are described. The main fact is that we are using viscous Navier-Stokes equations on hybrid meshes with structured and unstructured mesh part in the computational domain with conformal or non-conformal interfaces between domains. This is a powerful technology with high flexibility for mesh generation of interacting sails for two and three-dimensional flows.

Governing equations

The flow simulations around interacting sails presented in this paper are based on the numerical resolution of the following Reynolds Averaged Navier-Stokes equations:

$$\frac{\partial \rho}{\partial t} + \frac{\partial}{\partial t}(\rho u_i) = 0$$

$$\frac{\partial}{\partial t}(\rho u_i) + \frac{\partial}{\partial x_i}(\rho u_i u_j) = -\frac{\partial p}{\partial x_i} + \frac{\partial}{\partial x_j}[\tau_{ij} + R_{ij}]$$

With the viscous stress tensor

$$\tau_{ij} = 2\mu\,[S_{ij} - \frac{1}{3}\frac{\partial u_k}{\partial x_k}\delta_{ij}]$$

the deformation tensor

$$S_{ij} = \frac{1}{2}(\frac{\partial u_i}{\partial x_j} + \frac{\partial u_j}{\partial x_i})$$

and the turbulent Reynolds stress tensor R_{ij} which should be modelled (see turbulence modelling part). Following Boussinesq hypothesis this tensor may be approximated by:

$$R_{ij} \cong \mu_T\,[S_{ij} - \frac{2}{3}\frac{\partial u_k}{\partial x_k}\delta_{ij}] - \frac{2}{3}(\rho k)\,\delta_{ij}$$

Solver

The software package used to resolve the Navier-Stokes equations is Fluent 6. It is a steady or unsteady, compressible or incompressible, three-dimensional solver which resolve the previously given Reynolds Averaged Navier-Stokes equations. In the simulations presented, we have used the segregated solver and mainly the Spalart-Allmaras turbulence model in its vorticity-based or strain-vorticity-based production term. When not explicitly specified, second-order spatial and temporal schemes were used in the steady version.

To solve the Navier-Stokes equations proper boundary conditions are required on all calculation domain frontiers. At wall boundary, the no-slip condition is applied. A pressure outlet boundary condition is applied at the outlet. A velocity inlet boundary condition is applied on other frontiers (inlet, up and down).

Mesh issues

The mesh generation is a crucial step in the process of RANS simulation for many reasons. First of all, it is a time consuming activity which need engineer experience and long practice to rigorously clean the CAD geometry and do the best choice for the mesh topology. Secondly, the mesh influence on results on typical sails configurations is really important and should be carefully evaluated and bounded by relevant choices in mesh size in the important flow regions. Boundary layers have to be well resolved on all bodies (mast and sails) and this impose a critical criterion on mesh size in the normal direction to walls. But this well-known criterion is not enough to have a good flow description and results independent to mesh. All flow gradients have to be well resolved and this is not a simple task on typical sails because of the zero thickness and the subsequent leading-edge pressure gradient when angle of attack is not ideal.

In fact, it is good to know that results are never totally independent to the chosen mesh as opposed to what is frequently argued. The relevant question when interpreting RANS results on sails is: how bounded is the mesh influence on interesting results.

To illustrate the mesh convergence, figure 1, we have shown the lift-to-drag ratio convergence with mesh number of points on a typical sail (f/c = 12.5%, Re = 1.4 x 10^6) calculated on four meshes. We may see a good convergence of this critical performance parameter with the mesh number of points.

Another important feature of mesh is their adaptability or flexibility to be used with different kind of sail geometries and trim angles. A critical point for yacht rig aerodynamic studies is the necessity to generate meshes on multiple bodies (mast, mainsail, jib, etc…) which interact and may be displaced relative to others. The challenge is to generate good quality meshes in the boundary layers regions of each body without using too high aspect ratio cells and with a good control in the interaction regions which may be smalls (mainly between mainsail and jib in upwind sailing conditions as may be seen on figure 2, 3, 4). To respect these topologic constraints and obtain good mesh control, a good candidate is hybrid meshes

(as may be seen on figure 2) with eventually non conformal interface between the inner structured region around masts and sails and the outer unstructured region around all interacting structured domains (figure 2) as was done with Gambit 2.2 [7]. The mast trailing-edge with link to the zero-thickness sail is a region of difficulty for the structured mesh part and need much more attention and some tricks. Another interesting solution illustrated on figure 3 was to use unstructured fully hexahedral meshes with Hexpress [9].

Transition & turbulence modeling

A reliable prediction of the boundary layer transition through computer simulation is always a challenge today. The transition of a boundary layer is a highly complex physical phenomenon. It is a problem of stability of the Navier-Stokes equations which are highly sensitive to background turbulence level, pressure gradient, surface roughness, etc… The range of existing transition prediction methods extends from simplified empirical relationships through those based on linear stability to direct numerical simulations. All of these methods have critical limitations. No transition models are implemented in RANS simulations. Eventually transition may be tripped when transition location is known.

In the same time, mast and sail aerodynamic is highly concerned with separation bubble, turbulent transition and turbulent reattachment process and it is well known that these phenomenon and their associated pressure losses may have critical influence on pressure and friction distribution on sails. Also an accurate representation of laminar and turbulent separated flow regions is critical when we are concerned with drag prediction.

Despite this, we will see in this paper that a simple low cost turbulence model like the Spalart-Allmaras one may have coherent qualitative behaviour on mast-sail geometries and may reveal to be better than more sophisticated ones.

The Spalart-Allmaras turbulence model used is a one equation model with standard coefficients values. The equation is a transport equation for the turbulent viscosity as follow:

$$\frac{\partial}{\partial t}(\rho\tilde{\nu}) + \frac{\partial}{\partial x_i}(\rho\tilde{\nu}u_i) = P + Diff - Diss$$

$$P = C_{b1}\rho\tilde{S}\tilde{\nu}\,,\ \tilde{S} \equiv S + \frac{\tilde{\nu}}{\kappa^2 d^2} f_{\nu 2}\,,\ f_{\nu 2} = 1 - \frac{\chi}{1+\chi f_{\nu 1}}$$

$$Diff = \frac{1}{\sigma_\nu}\left[\frac{\partial}{\partial x_j}\left[(\mu+\rho\tilde{\nu})\frac{\partial\tilde{\nu}}{\partial x_j} + C_{b2}\rho\left(\frac{\partial\tilde{\nu}}{\partial x_j}\right)^2\right]\right]$$

$$Diss = C_{w1}\rho f_w\left(\frac{\tilde{\nu}}{d}\right)^2$$

$$\mu_T = \rho\tilde{\nu}f_{\nu 1}\,,\ f_{\nu 1} = \frac{\chi^3}{\chi^3 + C_{\nu 1}^3}\,,\ \chi = \frac{\tilde{\nu}}{\nu}$$

$$S_{vorticity-based} \equiv \sqrt{2\Omega_{ij}\Omega_{ij}}\,,\ \Omega_{ij} = \frac{1}{2}\left(\frac{\partial u_i}{\partial x_j} - \frac{\partial u_j}{\partial x_i}\right)$$

$$S_{strain-vorticity-based} \equiv \left|\Omega_{ij}\right| + C_{prod}\min(0, \left|S_{ij}\right| - \left|\Omega_{ij}\right|)$$

$$C_{prod} = 2\,,\ \left|\Omega_{ij}\right| \equiv \sqrt{2\Omega_{ij}\Omega_{ij}}\,,\ \left|S_{ij}\right| \equiv \sqrt{2S_{ij}S_{ij}}$$

$$f_w = g\left[\frac{1+C_{w3}^6}{g^6 + C_{w3}^6}\right]^{1/6}\,,\ g = r + C_{w2}(r^6 - r)\,,\ r = \frac{\tilde{\nu}}{\tilde{S}\kappa^2 d^2}$$

$$C_{b1} = 0.1355, C_{b2} = 0.622, \sigma_\nu = 2/3, C_{\nu 1} = 7.1$$

$$C_{w1} = \frac{C_{b1}}{\kappa^2} + \frac{1+C_{b2}}{\sigma_\nu}, C_{w2} = 0.3, C_{w3} = 2.0, \kappa = 0.4187$$

INTEGRATED & AUTOMATED COMPUTATIONAL ENVIRONMENT

Because fluid motion around interacting sails in their real environment is complex with separated flow regions, unsteady phenomena, because there are a lot of parameters that define a sail design or a complete rig design, there is a crucial need to integrated and automate the entire simulation process to be used during the design process in a reasonable turnaround time. This will give us the ability to analyse large number of configurations and design. This will open new way to design and optimize fluid motion around interacting sails.

Because, we think that it was a central question for the usefulness of RANS simulations in yacht design, we have developed a new tool able to integrate and automate the entire computational environment of RANS flow simulation from CAD definition, to mesh generation, flow simulation, flow analysis and design modifications through optimization following the diagram of figure 5. The main difficulty has been on mesh generation automation. But when the problem has been resolved, it has been obtained a tool with a high reliability through high mesh similarities between configurations. This has increased the ability to compare and rank different design or sail trim.

As it will be shown through examples, with *ADONF*, it becomes possible to investigate and

resolve new questions about fluid motion around designed bodies and their related performances.

The first level of questions is “what-if” questions. What will be the performance of this rig design if I change the mast section? What will be the performance of this rig if I change the sail recovery factor preserving a constant sail surface? Etc... Next, with the implemented optimization algorithms in *ADONF*, a second, higher level, ensemble of questions becomes open to the designer. How to change the rig design or the deck plan to increase the performance of the sailing boat in given wind conditions? How to change rig trimming to increase boat speed in given wind conditions? What is the best camber and trim of these two interacting sails to maximize driving force or driving to heeling force ratio? Etc…

RESULTS

Few examples will be chosen to illustrate the sort of design questions open by *ADONF*. Many interacting sails problem will be considered. Most sailing boats use two or more interacting sails and Hydraplaneur use windward/leeward interacting sails. These interactions between soft sails are a complex design challenge with many unresolved questions.

As the classical sails interaction problem, the interaction of mainsail and jib is a well known problem of sailing yachts with a long history of debate and controversies amongst sailing community [12]. Those who analyse this interaction as a venture effect between both sails and those who speak of a slotted mainsail with a jib. The problem has been largely clarified by Arvel Gentry in his famous article in 1971 [8]. He explain that the slot effect between the jib and the mainsail result in a velocity decrease in the gap and not in a velocity increase, comparatively to a mainsail alone, as was said before by invoking the Venturi effect. These clarifications were obtained by using potential inviscid methods (experimental and numerical). It is interesting to come back to this problem by using viscous methods and see if more understanding can be obtained on this interaction problem.

In these investigations, we will focus our attention on sail camber and sail trim angle influence on interacting sails.

The first section illustrates the necessity of viscous methods in downwind sailing conditions but also in upwind conditions. The second section presents the optimization of a single sail, to have a reference case. Then the following sections illustrate interacting sails problems.

Inviscid versus RANS prediction

In the fluid mechanics community, many people know that inviscid methods and viscous/inviscid coupling methods through integral boundary layers are limited to non separated flows and should be used with great caution to do not put forward misleading conclusions about sail design [4, 5,10,11,14]. Today, RANS equations are the more general model to predict unsteady turbulent flows with separated regions. Drawbacks of this model are computing time and mesh generation. With the continuous increase of computing power, computing time will not be a problem for a long time. Today, one 2D RANS simulation around two sails with a fine mesh is about twenty minutes on a laptop. Mesh generation for two-dimensional simulations is no more a problem. The hybrid approach used here well adapted and highly flexible to generate meshes with a good boundary layer description along sails with a structured mesh and unstructured mesh to assemble all sails meshes. Three-dimensional meshes remain a difficult task to obtain reliable results with a good description of sails boundary layers and atmospheric boundary layer description and transport along the computational domain but these issues need to be addressed.

Contrary to what is frequently said, separated flow regions are not reserved for downwind sailing conditions. It is a simplistic point of view. Separated regions are generally smallest in upwind sailing conditions with well trimmed sails but they may greatly influence drag and then also the lift-to-drag ratio. In all sailing conditions, the mast at the leading-edge of the mainsail will create a separated flow region which will greatly increase the total drag in a non-linear fashion [5,14]. In this context, we have shown that well used RANS methods with carefully generated meshes are able to give a good qualitative description of the main flow features, as may be seen on figure 6, and predict realistic performances compared to experimental data [5,17-19].

In the same manner, high camber sails like code x or gennaker are submitted to flow separation in their useful range of incidence angle as shown in figure 7. As can be seen, the flow around a gennaker at its ideal incidence angle will probably be separated in some regions with unsteady vortex shedding. These unsteady flow features may have consequences on performances of high camber sails. These sails are used for a large range of apparent wind angle (nearly 45° to 145°) with high angle of attack. Unsteady RANS methods may be used to model and predict these unsteady separated flows. An illustrative example is shown in figure 8 with vortex shedding prediction behind a gennaker with 30% camber. A comparison of the predicted maximum lift coefficient on high camber sails with coupling inviscid/viscous methods [16] and with RANS methods is shown in figure 8. Both methods agreed for moderate camber sails but

differences are increasing with sail camber when it is higher than 8 to 9%. RANS or URANS model are needed to predict flows around high camber sails like gennaker in reaching and downwind sailing conditions where separation and unsteadiness are commonplace. Large performance increase may be obtained on these high camber sails [1]. This will be further illustrated in a following section.

Sail design optimization

To evaluate optimization methods included in the *ADONF* package, we will look at a mixed optimization (design & trim) problem on a single sail. We take a sail in a wind and let its camber and sheeting angle as optimization variables used to maximize the driving force F_r first and then the driving to heeling force ratio F_r/F_h. Both objectives functions main be useful for different wind and sailing conditions [12]. The data are the following:

Table 1: data of the sail optimization problem

β	x_f	C	f_0	δ_0
30°	30%	6500	7%	13°

The apparent wind angle is β = 30° corresponding to upwind sailing. The sail camber and sail trim angle (δ, f/c) which was found to maximize the driving force, through the optimization process was a sheeting angle of δ=20° and a sail camber of f/c=18% (Table 2). The optimization algorithm used was the simplex method (Sim). In a second time, we have resolved the same optimization problem with a genetic algorithm (GA) recently implemented in *ADONF*. We found nearly the same optimum values for sail camber and trim angle (see table 2). More tests have shown that the optimum found with genetic algorithm may be dependent to the size of the population used. This result will be investigated in more details in a future paper with a newer multi-objective genetic algorithm implementation. We have also verified that the simplex algorithm which need an initialization of the sail camber and trim angle values to begin the optimization process was able to found a single converged optimum independent to the initial solution.

Table 2: optimum results

Objective	Method	f_{GV}	i_{GV}
Max(Fr)	Sim	18%	10°
"	GA	18%	8°
Max(Fr/Fh)	Sim	6.8%	2.5°

Flow streamlines around this optimum sail design and trim is represented on figure 10. We may remark that the flow around a single sail which maximize its propulsive force as computed by RANS model is not fully attached. A trailing-edge separation region is clearly seen on the leeward side of the sail.

In the same manner, the sail camber and trim angle couple (δ, f/c) which maximize the driving to heeling force ratio, through the optimization process was a sheeting angle of δ=28° and a sail camber of f/c=7%. With this second computed optimum, we found a well known result. To maximize the aerodynamic finesse or lift-to-drag ratio of a sharp leading-edge sail profile, we should use its ideal incidence angle. Flow streamlines around the sail are fully attached as may be seen on figure 11. In this particular case, without flow separation, inviscid methods will probably gave similar results to those obtained here with RANS methods.

Interacting sails optimization

Knowing the optimum camber and sheeting angle of a single sail, as predicted by RANS model, it was interesting to investigate how the optimum will be changed by the interaction of sails. Sailors know that sail design optimums are different on a real yacht when we are considering a single sail or a combination of a mainsail and a jib for example.

To investigate the ability of *ADONF* software package to capture realistic optimum for sails camber values and sheeting angles values, we have search for the optimum driving force and driving to heeling force ratio of a mainsail and a jib interacting by running RANS flow simulations on a collection of mainsail-jib configurations following the implemented simplex optimization algorithm. On figure 10, we see flow streamlines around sails which maximize driving force on a single sail on the top and on a mainsail-jib rig on the bottom. We clearly see that both flows include separated flow regions on the upper surface at the trailing-edge. This is a classical result for sail design which maximizes driving force. An interesting result obtain through the optimization process and shown on figure 10 is the highest sail camber values found on the mainsail-jib rig compared to those found on a single sail. We found 18% for a single sail and 27% and 30% for interacting mainsail-jib (Table 2 & 4). This shows the benefit of interacting sails with a front one (jib) in the leeward side of a rear one (mainsail) in the windward side. With the positive interaction between mainsail and jib it is possible to design highest camber sails to increase the resultant propulsive force for a given sail surface. This result is probably known by sail designers. Here, it is found through an automated optimization process of RANS-based simulations.

In the same manner, on figure 11, we see flow streamlines which maximizes driving to heeling

force ratio on an optimum design and trim of a mainsail interacting with a jib. As before, camber optimums are smaller than for maximizing the propulsive force as we may anticipate. In these optimum flows, because we search for a high finesse, we obtained a well behave streamline pattern around both sails without any separated flow regions. As in the previous case, we see that the jib may have a higher camber when interacting favorably with a mainsail. The optimum sail camber was around 7% for a single sail and is 4% for the mainsail and 19% for the jib in the interacting mainsail-jib configuration. This interacting sails optimum was not anticipated but seems in agreement with today sail design of competition sailing boats. It will be interesting to share these RANS-based optimums with sail designer experiences and to try to extend the optimization search to three-dimensional parametric rigs in the future. Figure 12 shows the pressure coefficient distribution along the jib with and without the presence of the mainsail. It is clearly seen that on this optimized design and trim, the mainsail presence is highly beneficial to the propulsive force generated on the jib. Without the mainsail, the jib is separated along its windward side with nearly zero lift generated on that side. In the same way we may note the presence of a small separation region in the leeward side near the trailing-edge with a constant pressure region. In the presence of the mainsail, all separation regions of the jib have disappeared and the jib loading was greatly increased. This clearly confirms A. Gentry analysis about mainsail-jib interaction [8].

These examples of interacting sails, have illustrated the benefit which may be obtained with a viscous flow simulation and optimization tool to better understand, design and trim flows around interacting sails.

Table 3: data of the mainsail-jib optimization problem

C_{GV}	C_{JIB}	xf_{GV}	xf_{JIB}
6500	6250	30	40

Table 4: optimum design & trimming results

Objective	f_{GV}	i_{GV}	f_{JIB}	i_{JIB}
Max(Fr)	27%	27°	30%	-2°
Max(Fr/Fh)	4%	20°	19%	-1°

Hydraplaneur double rig optimization

ADONF has been applied to the double rig of the Hydraplaneur of Y. PARLIER (figure 16) to do analysis and optimisation of this new rig concept.

Two-dimensional analysis of the double rig

One of the main aerodynamic design objectives of the double rig was to increase sail surface without increase of the heeling and pitching moments. The known disadvantage of this rig is the blanketing effect of the windward rig over the leeward rig when apparent wind angle increase. This double rig phenomenon was first illustrated (figure 13) and measured during wind-tunnel tests [4,6]. Through these tests, it as been possible to determine the range of apparent wind angle where the double rig generate more driving forces than the single one with a given heeling moment. In a second part, we have used viscous CFD to determine the flow pattern around the double rig in the critical range of the apparent wind angle in reaching conditions. Objective was to propose solutions to extend as much as possible the flight domain of the double rig through relevant design choices. Also, we have chosen to study a typical sails configuration, for reaching conditions, with the two mainsails and a small gennaker in the leeward side.

Before running multi-objective optimization on complex interacting sails, to be able to increase driving force without increase of the heeling moment, we have done RANS simulations on a large number of sails trimming configurations for the three sails, to explore the trimming space. We have represented an example of these trimming conditions for two mainsails and a gennaker on figure 14. This first investigation aim at representing response surfaces of the optimization problem to know their properties and select the more relevant optimization algorithm. Following the response surfaces properties it may be better to use simplex, gradient-based or evolutionary algorithms.

Because in our three-dimensional space, it is not possible to visualize response surfaces with more than two parameters, we have chosen to represent the propulsive force of the double rig as a function of the trim angles of the two mainsails as an example on figure 15. This response surface was obtained by running forty RANS simulations. It takes approximately two nights on a laptop. As a first result, we see that this response surface is not monotonous. There are local optimums and one global optimum. As a consequence, we may say that classical gradient-based algorithms will not be appropriate to find the global optimum of this kind of RANS-based optimization. Genetic algorithms should be more appropriate for this task and its extension to constrained multi-objective problems. We are currently implementing a newer multi-objective genetic algorithm in *ADONF* to extend the optimization capabilities.

These results and some others three-dimensional RANS simulations have been used to propose new rig design solutions to increase the double rig efficiency by increasing the critical apparent wind angle.

Three-dimensional analysis of interacting sails

We know that 3D RANS simulations are absolutely necessary for analysis, design and optimization of interacting sails because span lift distribution is not uniform along sails and result in induced drag effect which cannot be modelized by 2D RANS. Moreover, atmospheric boundary layer over sea surface create a velocity profile $V_{TW}(z)$ and composed with boat speed V_B result in an altitude variation of the apparent wind speed $V_{AW}(z)$ and wind angle $\beta_{AW}(z)$ (see equations). To take this into account in sail design, sails are twisted to adapt angle of attack of each sail section along span with apparent wind angle variation. This atmospheric boundary layer effect is particularly important in downwind sailing conditions because twist is larger than in upwind sailing conditions. To take these phenomena into account, we are developing an extension of *ADONF* to full three-dimensional rig configurations.

Simulations of full three-dimensional flow field around Hydraplaneur double rig have been done with atmospheric boundary layer effect. Geometry used includes two wingmasts, two mainsails and eventually arms of the boat. Two flow conditions were used with 15 knots of true wind speed. The first one corresponding to upwind conditions with an apparent wind angle of 25° and the second one to reaching conditions with an apparent wind angle of 56° at altitude z=10 meters above the sea level. Upwind and reaching simulations were done with a turbulent atmospheric boundary layer profile following:

$$V_{TW}(z) = V_{TW}(z_{ref})[z / z_{ref}]^{1/7}$$

$$\beta_{AW}(z) = Arctg[\frac{V_{TW}(z)\sin\beta_{TW}}{V_B + V_{TW}(z)\cos\beta_{TW}}]$$

Actually, it is easy to take into account the wind vertical gradient and twist in three-dimensional RANS based simulations through an inlet boundary condition with a specified velocity profile ($V_{AW}(z)$, $\beta_{AW}(z)$). Investigations of the influence of the atmospheric state (laminar or turbulent) on the rig performance will be easy to do. The real difficulty is to transport the atmospheric boundary layer profile from the inlet of the computational domain to the boat location without smearing (Figure 17-19).

Studies have been done to define a velocity profile transport criteria to determine relevant mesh size properties during the mesh generation to capture atmospheric boundary layer with sufficient accuracy (Figure 17-19). Different mesh topologies were tested during this process to determine the more efficient choice between computing time to obtain a converged solution and accuracy of the wind vertical gradient and twist at the boat location after its transport along the flow domain.

Extend of the computational flow domain was approximately 70 sail chord in both horizontal direction and 3 mast height in the vertical direction (Figure 17). Numerous unstructured and hybrid meshes were generated before to found the best compromise.

Upwind sailing

In upwind sailing condition, the first coarse mesh used was composed by approximately 544 000 tetrahedral elements. The meshed Hydraplaneur geometry takes into account the heel, the inward and rear angles of masts. It was used to do first 3D RANS simulations around the Hydraplaneur with transverse beams as shown on figure 20. These simulations were used to characterize the three-dimensional flow pattern in the lower part of the rig to understand interactions with transverse beams and evaluate their impact on the sails aerodynamic. This gives first estimates of the pressure drag component of beams relative to the total aerodynamic drag.

In a second time refined meshes were used to increase accuracy of masts and sails boundary layer prediction. The best volume mesh used for upwind conditions contain 1 977 000 elements with 60 000 surface elements on sails, 80 000 surface elements on masts. Figure 21 shows a view of the flow field in upwind sailing conditions. Tip vortical structures at both ends of sails in the aft cut plane are always clearly seen on the rear plane coloured by total pressure. We see that the lower vortical structure is stronger than the higher one. An examination of the static pressure field on windward and leeward rigs shows that the leeward rig is more loaded that the windward one. This differential loading results in a lift coefficient ratio Cl_1/Cl_2 of 1.3 in this attitude. To equilibrate the yaw moment, it will be necessary to use differential sheeting angle for each mainsails. Then a question rise: how to equilibrate windward and leeward loading? What is the right solution to reduce induced drag? The induced drag of the double rig may be decomposed following this expression:

$$C_{di} = C_{di\_windward} + C_{di\_leeward} + C_{di\_interaction}$$

Through an inviscid lifting-line analysis it is possible to show that differential loading should be annulated by a correct trimming of sails, to minimize induced drag as shown by von Mises in 1959 [15].

Is it true for real flows? We have noted that sheeting angles are generally different in the leeward and windward side of the Hydraplaneur at sea. Is it to equilibrate yaw moment or to reduce induced drag? Is it possible to obtain both with the same trimming? Three-dimensional viscous CFD may be used to gain insight into this important design question for double rig and increase our ability to design it.

Downwind sailing

Full three-dimensional RANS-based simulations are particularly well adapted for reaching or downwind sailing conditions for many reasons. Sails used in these conditions like gennaker or code x are high camber sails, angles of attack are higher than in upwind sailing, atmospheric boundary layer twist angle variation is higher, and flows are frequently separated in some regions with unsteady phenomenon such as vortex shedding at sail leading or trailing-edge.

The Hydraplaneur double rig open new questions about sail design because sail designers are not familiar with this kind of sails interactions. There is not much more experience about double rig sails design.

To investigate these new questions we have done simulations in reaching conditions with an apparent wind angle of 56° at 10 meters above the level sea.

A relevant question immediately rises when we have obtained three-dimensional flow results: how to visualize main flow features to understand the flow and to guide design modifications? Figure 22 is an illustration of what can be done in flow visualization to understand the complete flow pattern in full three-dimensional RANS simulations. We have represented sail surfaces with mesh surfaces to have a well apprehension of the sail twist and volume. To visualize separated flow regions, we have represented low speed regions in eleven cut plane parallel to sea surface along sail span. This seems good to represent cross stream and streamwise extension of separated regions. To visualize tip and bottom vortex, we have introduced air stream strip in front of the rig. These strips are cut by sail surfaces and distorted by cross stream velocity component to form tip and bottom vortex which generate induced drag. In this simulation, the windward and leeward rig sheet angles are 35° and 30°. It is seen on the figure 22 that despite the 5 ° reduction of the angle of attack of the windward rig compared to the leeward one, separation region is always larger on the windward rig. This is another illustration of the differential loading between each rig which is a particularity of the double rig. If we are looking for the driving force distribution on sails for two trimming, we found the following table:

Table 5: driving force distribution on two trimming of the double rig with β=56°
C1: δ_{GV1} = 30°, δ_{GV2} = 30°
C2: δ_{GV1} = 35°, δ_{GV2} = 30°

	Windward Lower	Windward Upper	Leeward Lower	Leeward Upper
C1	4.8	5.7	4.1	9.5
	44%		56%	
C2	5.2	6.8	4.3	8.7
	48%		52%	

Several remarks may be drawn from the table 5.

First, on both trimming, we see that sail surfaces which are in front of the other rig (Windward upper surface and leeward lower surface) have a decreased contribution to the driving force compared to other sail surfaces (Windward lower and leeward upper). These losses of efficiency of inward surfaces of the double rig are directly related to mainsails interaction. This is the inconvenient side of double rig but it is not all about the double rig. There is also an advantage side we will see later.

Second remark, the only difference between each trimming is an increase of the mainsail sheeting angle of the windward rig on the second trimming. Consequences of this larger mainsail sheeting angle of the windward rig have consequences on both mainsails. When we ease the windward sheet by 5°, we note an increase of the driving force contribution of that sail by 1.5 (+0.4 on the lower side and +1.1 on the upper side) but this is accompanied by a decrease of the driving force contribution of the leeward sail by -0.6 (+0.2 on the lower side and -0.8 on the upper side) which results in a net increase of 0.9. This emphasizes the sails interaction and coupling mechanisms which take place during the trimming of sails of the double rig and the associated difficulty to find the best trimming. Viscous CFD when integrated in a complete automated environment with CAD, mesh generation, solver and post-processing, are very helpful to increase our understanding of these complex rigs with coupling mechanisms.

CONCLUSIONS

It has shown that emerge new methods to use viscous CFD based on RANS or URANS simulations useful for sailing yacht design. These methods are based on the ability to develop an automated computational environment. This environment includes the design, the mesh generation, the flow solver and the post-processing before to go through an optimization process based on relevant evolutionary or hybrid algorithms to

generate new optimal design based on designer choices about free variables and objective criteria. As before, the question is to pose the right questions to the design but now the designer may be aided by a new decision-making tool.

The software package *ADONF*, has been developed to be able to pose new questions about interacting sails design. Examples from the innovating double rig of the Hydraplaneur of Y. PARLIER have been used to illustrate the potential of *ADONF* to tackle interesting rig design problem and increase our sail flow physics understanding.

New results about interacting sails design and trimming has been obtained through two-dimensional and three-dimensional RANS-based simulations and optimizations with simplex and evolutionary algorithms. Through a problem of three interacting sails, it has been shown that RANS-based response surfaces may contain local optimums and a global optimum which imply the use of evolutionary algorithms to find the global optimum.

ADONF will be extended to full three-dimensional RANS simulations to try to extend obtained 2D results about interacting sails design and trim to 3D interacting sails. It will be also extended to multi-objective constrained optimization with a new genetic algorithm. This is necessary to do optimization with constrained heeling moment.

Another planned development is to enhance sail design ranking for a given yacht by coupling ADONF to a VPP.

But we should not forget that sails are soft materials. Also we must be aware to the needed development of a fluid-structure coupling strategy to be able to increase our control to the link between design shapes and flying shapes.

ACKNOWLEDGEMENTS

Authors wish to acknowledge J.B. Cazalbou for his help, H. Belloc, V. Allain, S. Lefèvre, G. Busnel, W. Richard for their support on the experimental part of this work, C. Palaysi for his support about computers and software and ENSICA for the support of this activity. This research was partly funded by Y. PARLIER – Hydraplaneur Médiatis Région Aquitaine project.

REFERENCES

1. Burns Fallow J., America's Cup sail design, J. of Wind Engineering and Industrial Aerodynamics 63, 1996, p183-192.
2. Caponnetto, M. and Castelli, A. "America's Cup Yacht Design using Advanced Numerical Flow Simulations", EPFL Super Computing Review, 10, Nov 1998.
3. Caponnetto, M., Castelli A., Dupont P., Bonjour B., Mathey P.L., Sanchi S., Sawley M.L., Sailing Yacht Design Using Advanced Numerical Techniques, *14th Chesapeake Sailing Yacht Symposium*, Annapolis, Maryland, USA, March 1999.
4. Chapin, V. G., Neyhousser, R., Jamme, S. Dulliand, G., Chassaing, P. (2005), "Sailing Yacht Rig Improvements through Viscous CFD", *17th Chesapeake Sailing Yacht Symposium*, Annapolis, Maryland, USA, March 2005.
5. Chapin, V. G., (2005), "Viscous CFD as a relevant decision-making tool for mast-sail aerodynamics", *Marine Technology*, **42**(1), 1-10.
6. Chapin, V.G. (2002), "Gréement Gerris", Contract report n°2002-2.
7. Gambit 2.2, from FLUENT, http://www.fluent.fr/
8. Gentry, Arvel, (1971), *The Aerodynamics of Sail Interaction*, 3th AIAA Symposium on the Aero/Hydronautics of Sailing, November 1971.
9. Hexpress, from NUMECA International, http://www.numeca.com/
10. Jones, P., & Korpus, R., (2001), "International America's Cup class yacht design using viscous flow CFD", *15th Chesapeake Sailing Yacht Symposium*, Annapolis, Maryland, USA, January 2001.
11. Korpus, R., (2004), "Reynolds Averaged Navier-Stokes in an Integrated Design Environment", MDY04, Madrid, Espagne.
12. Marchaj, C. A., (1996), *Sail Performance*, McGraw Hill, Great Britain.
13. Milgram J.H., "Sail Force Coefficients for Systematic Rig Variations", September 1971.
14. Milgram J.H., "Effects of Masts on the Aerodynamics of Sail Sections", Marine Technology, vol. 15(1), 35-42, 1978.
15. Mises R. von, "Theory of flight", Dover 1959.
16. Norris, S. E. (1993), "The interaction of Yacht Sails in a Two-Dimensional Viscous Flow", *Master of Engineering*, University of Auckland, New-Zeeland, May 1993.

17. Wilkinson S., “Partially separated flows around 2D masts and sails”, PhD Thesis, University of Southampton, 1984.
18. Wilkinson S., “Static Pressure Distributions Over 2D Mast/Sail Geometries”, Marine Technology, vol 26(4), 333-337, 1989.
19. Wilkinson S., “Boundary Layer Explorations Over a 2D Mast/Sail Geometry”, Marine Technology, vol 27, 250-256, 1990.

APPENDIX

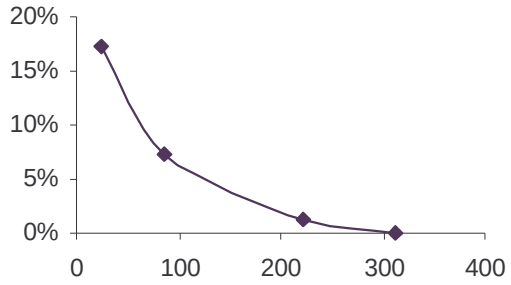

Figure 1: lift-to-drag ratio convergence with mesh refinement (number of points divided by 1000)

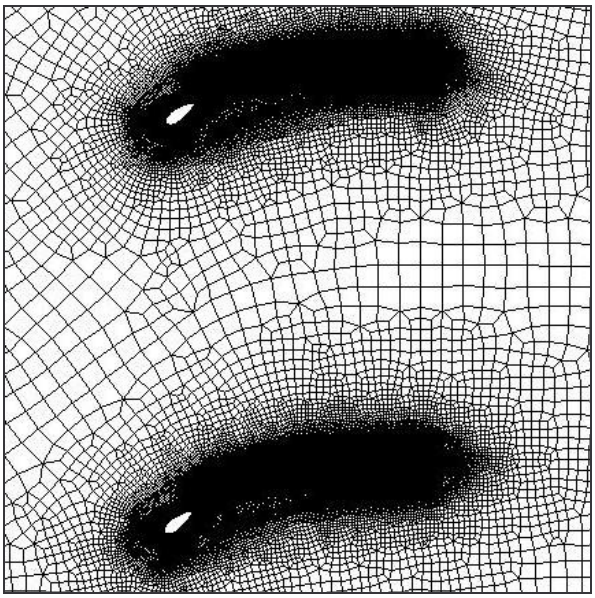

Figure 2: hybrid mesh example

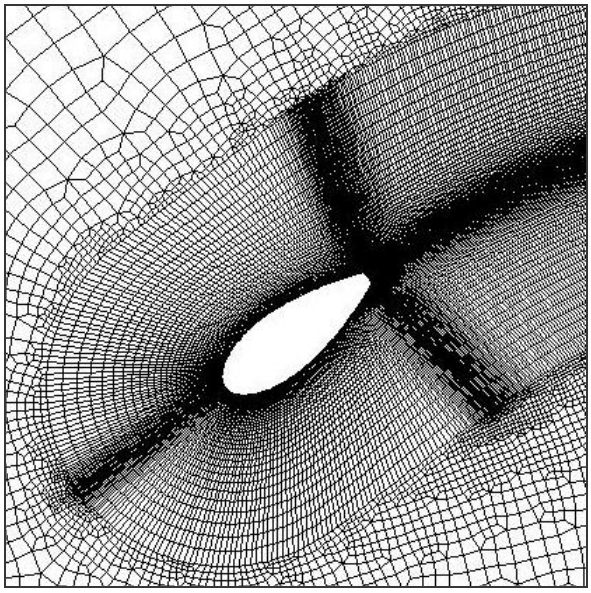

Figure 3: hybrid mesh zoom

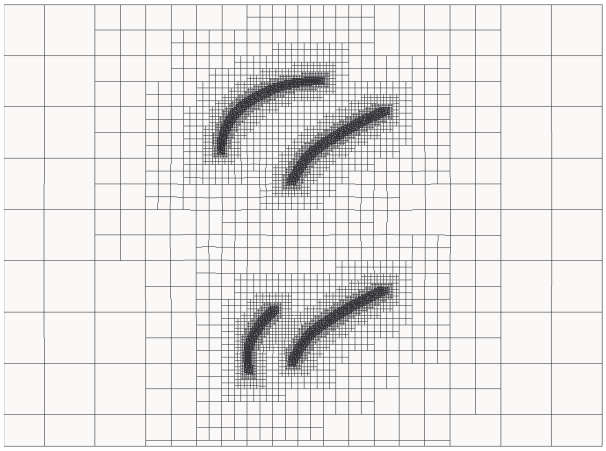

Figure 4: unstructured mesh around 4 interacting sails

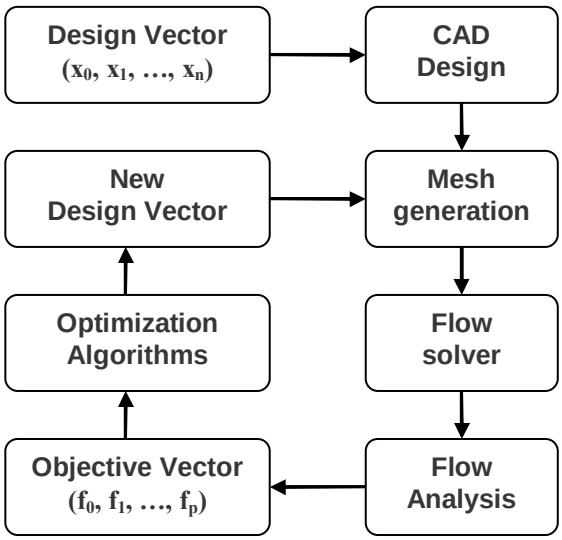

Figure 5: *ADONF* software package diagram

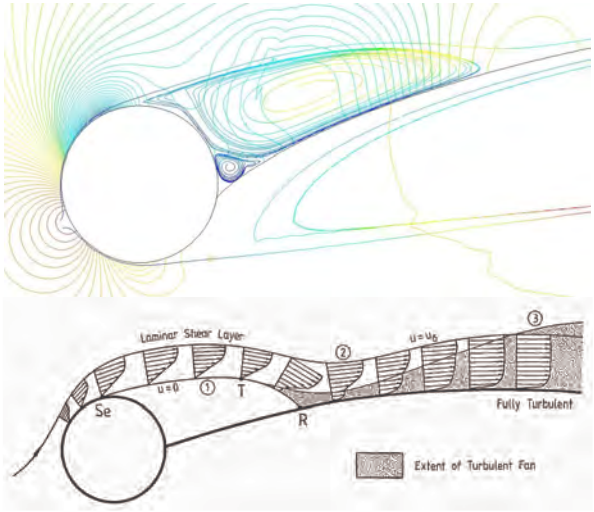

Figure 6: (a) RANS flow visualization (d/c=10%, f/c=12.5%, i=5°, Re=1.4 x 10^6). (b) Upper-surface.

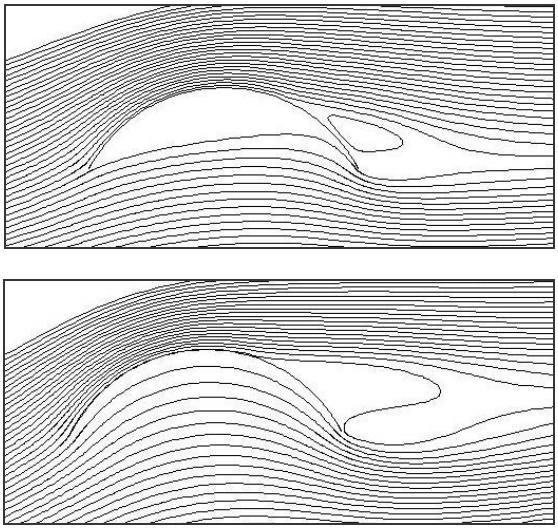

Figure 7: RANS prediction around high camber sails (a) ideal incidence angle, (b) maximum lift coefficient

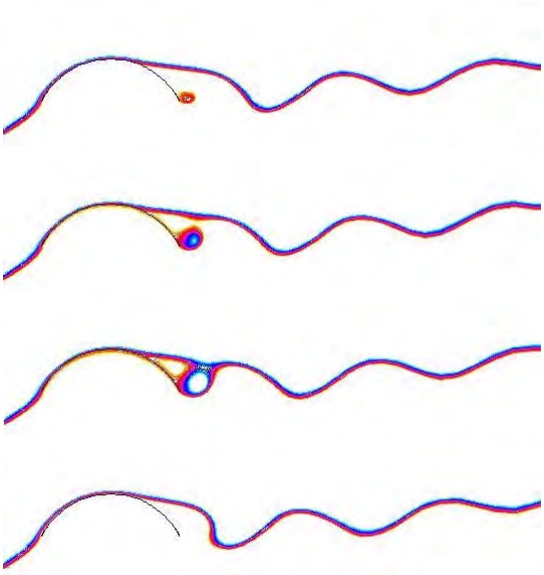

Figure 8: RANS prediction of vortex shedding on a high camber sail (4 instants in the period)

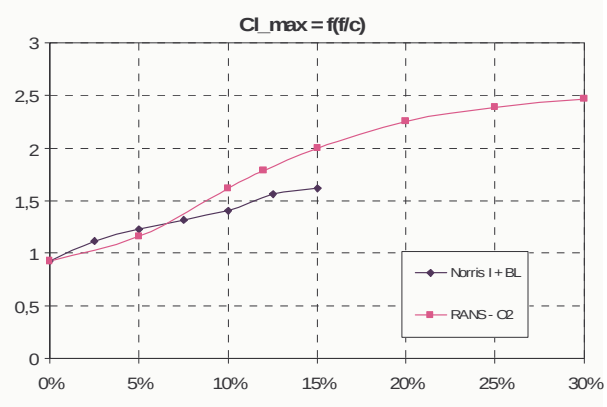

Figure 9: Inviscid/viscous coupling and RANS prediction of the maximum lift coefficient versus sail camber value f/c

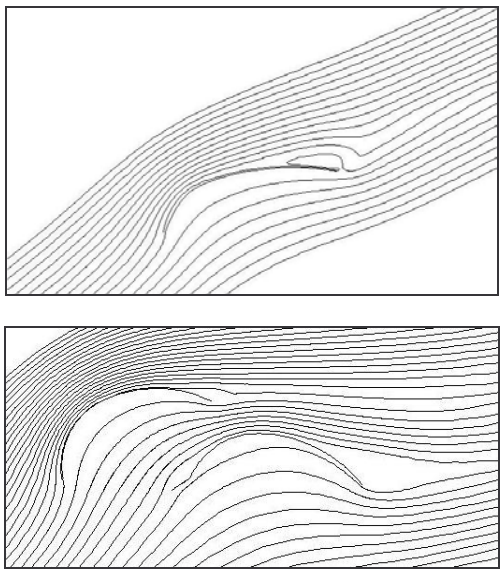

Figure 10: maximum driving force through optimum design and trimming. (a) mainsail alone, (b) mainsail-jib in interaction

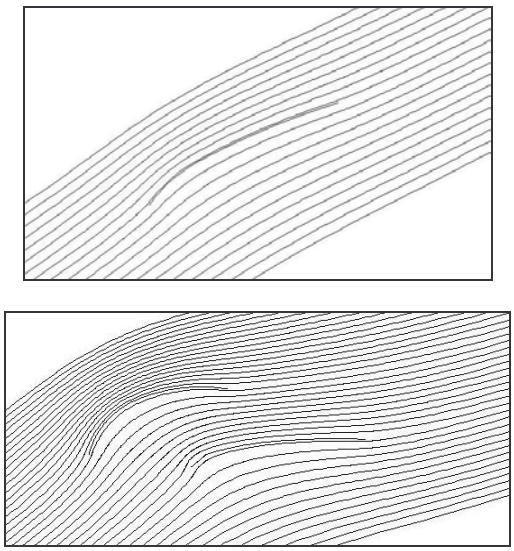

Figure 11: maximum driving to heeling force ratio through optimum design and trimming. (a) mainsail alone, (b) mainsail-jib in interaction

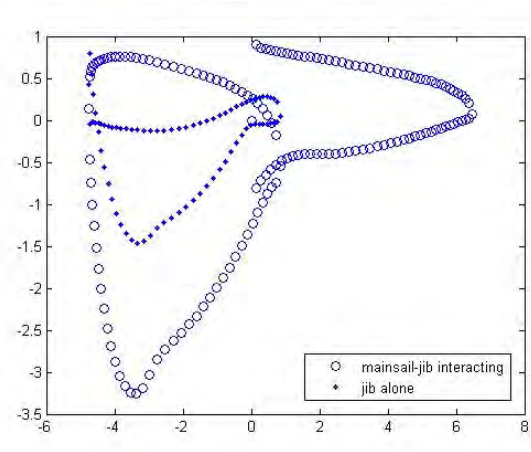

Figure 12: maximum driving to heeling force ratio through optimum design and trimming: pressure coefficient distribution

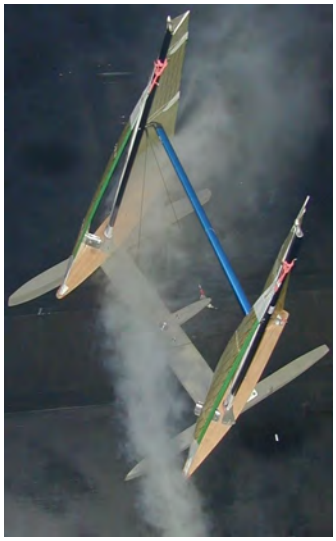

Figure 13: deviation of the air stream between the windward and leeward rigs.

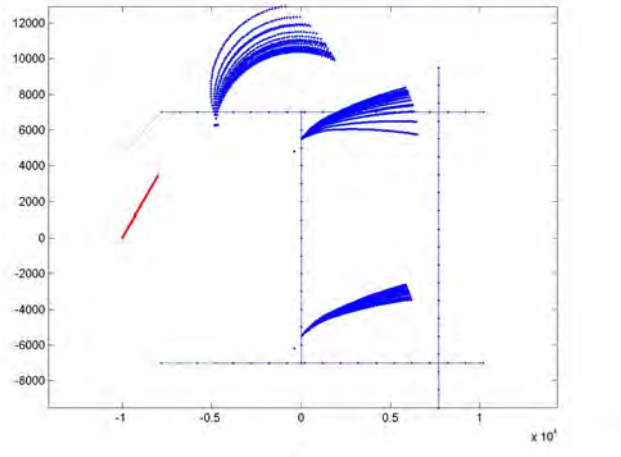

Figure 14: design and trimming exploration space of Hydraplaneur double rig in downwind sailing conditions

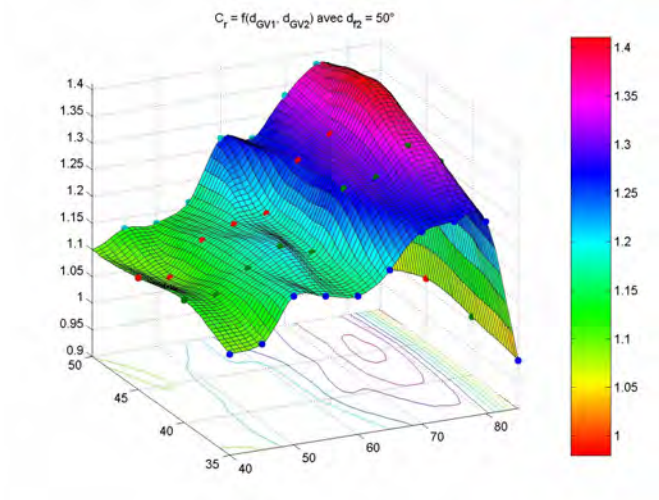

Figure 15: response surface of Hydraplaneur double rig in downwind sailing condition. Driving force versus mainsails trim angles

Figure 16: Hydraplaneur double rig of Y. PARLIER

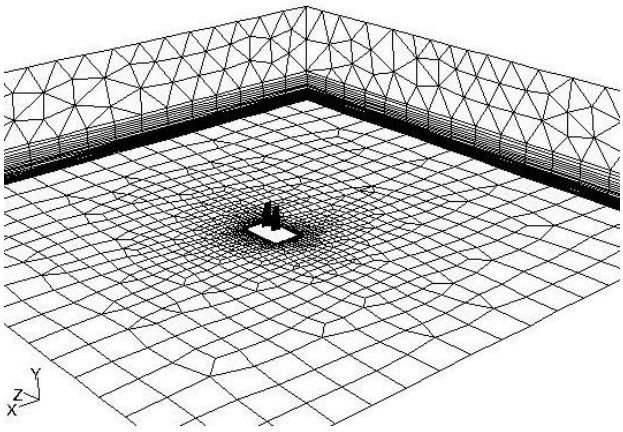

Figure 17: 3D mesh of Hydraplaneur double rig configuration for atmospheric boundary layer transport, 1.3 millions elements.

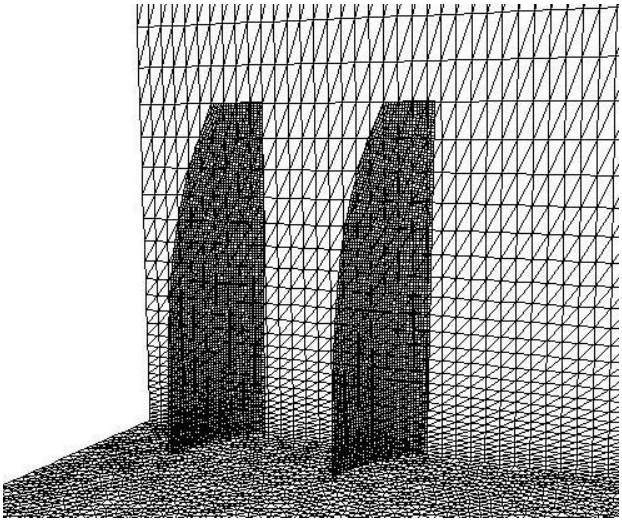

Figure 18: zoom in a 3D mesh of Hydraplaneur double rig, 1.3 millions elements.

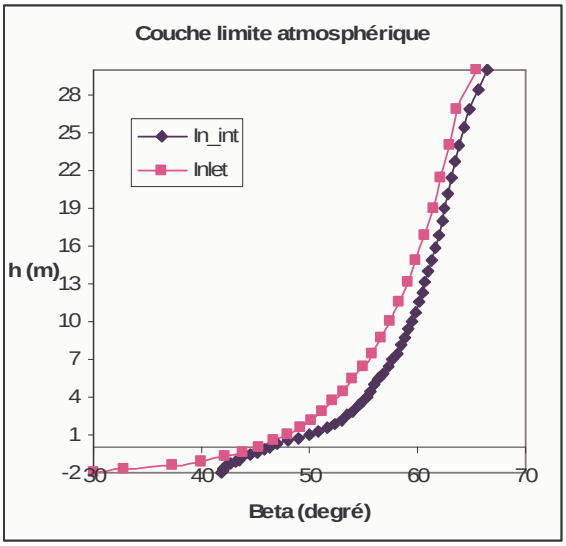

Figure 19: atmospheric boundary layer velocity profile transport from inlet to boat location

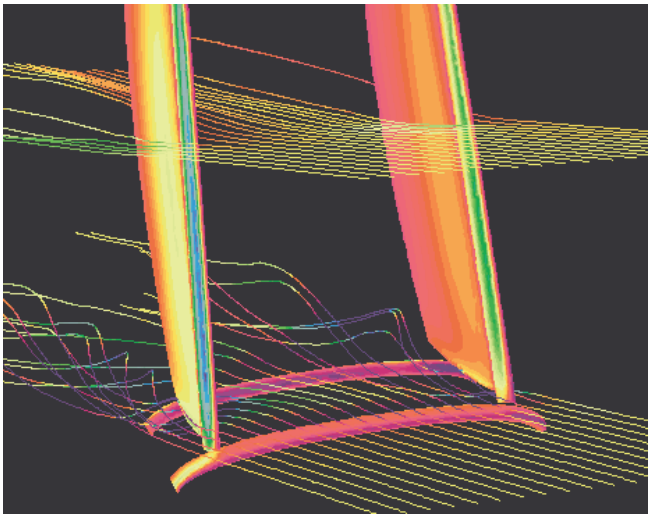

Figure 20: 3D RANS simulation around Hydraplaneur double rig in upwind sailing conditions

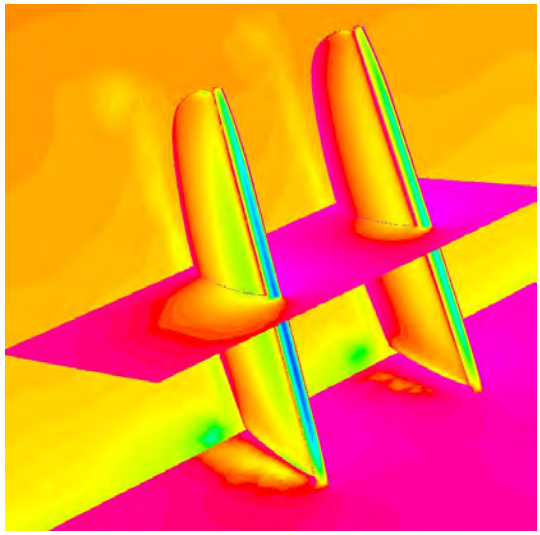

Figure 21: 3D RANS simulation around double rig in upwind conditions, 2 millions elements mesh.

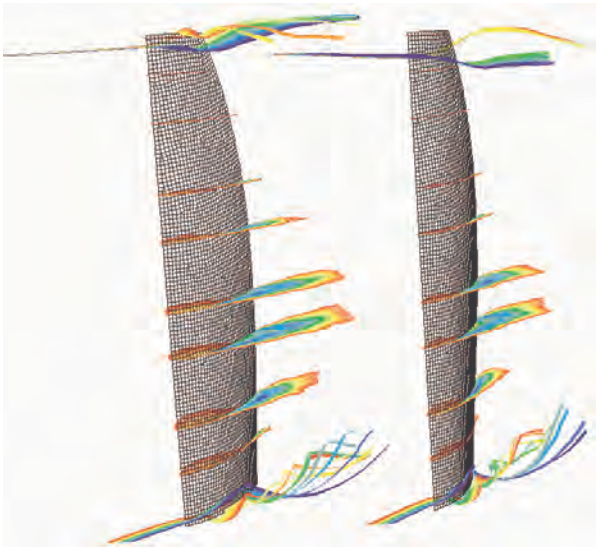

Figure 22: 3D RANS in reaching conditions β=56°, 1.3 millions elements mesh.